Proceedings of the Twenty-second (2012) International Offshore and Polar Engineering Conference
Rhodes, Greece, June 17–22, 2012

ISBN 978-1-880653-94–4 (Set); ISSN 1098-6189 (Set)
www.isope.org

Vortex-induced Vibrations of a Circular Cylinder with Different Geometric Disturbances

Lin Liming, Zhong Xingfu and Wu Yingxiang
Key Laboratory for Hydrodynamics and Ocean Engineering, Institute of Mechanics, Chinese Academy of Sciences,
Beijing, China

ABSTRACT

Based on previous works, experiments are carried out for effects of harmonic and cone-like disturbances on vortex-induced vibrations (VIV). The structures are designed as the pendulum oscillated transversely in water channel. Three waviness, the ratio of wavy height to the wavelength, of 0.025, 0.05 and 0.1 are presented with the non-dimensional prescribed wavelength of 6. With the increasing incoming velocity, the oscillating amplitude of the wavy cylinder is firstly decreased at the start of synchronization with the comparison to that of the straight cylinder, and then increased greatly at higher velocities. Meantime, the response region of the wavy cylinder is also enlarged with the comparison to that of the straight cylinder. Other characteristics of responses of amplitude and frequency at different incoming velocities are presented.

KEY WORDS: Vortex-induced vibration; circular cylinder; geometric disturbance; riser; experiment.

INTRODUCTION

Vortex-induced vibration of bluff body is an important phenomenon appeared in many engineering applications, such as higher buildings in architectures, marine risers or flexible pipelines in subsea production system, tubes in heat exchanger. Flow separation and associated vortex shedding behind bluff bodies lead to fluctuating fluid forces. Once the frequency of vortex shedding is close to the natural frequency of body, the synchronization is occurred, associate with the sudden magnification of oscillating amplitude and fluid force. This results in structural fatigue damage, sometimes even endanger safety of production and ocean environment for marine risers. Over a few decades, a large number of fundamental studies, including numerical simulations and experiments, have been conducted to understand the dynamics of VIV. Comprehensive reviews can be referenced in Sarpkaya (1979), Sarpkaya & Isaacson (1981), Sarpkaya (2004), Williamson & Govardhan (2004; 2008), and Gabbai & Benaroya (2005).

Accordingly, many control devices and methods in suppressing VIV have been proposed and applied in recent decades. Most of them were designed based on disturbing the flow past a bluff body, typically as a kind of passive control. For example, a spiraling arrangement of surface control bumps was proposed by Owen *et al*.(2001). Drag reduction can be reached up to 47%. The regular vortex shedding can no longer be detected at certain waviness. Control rods with equal space around cylinder, investigated by Song *et al*.(2009), can also reduce the transverse response of risers. So far, streamline fairing (Lee & Allen, 2005) exhibits very good aerodynamic performance due to its streamlined shape resulting in the bluff body streamlined and the delay of the flow separation. Furthermore, splitter plates can also effectively delay interactions between upper and lower free shear layers, as well as the formation of shedding vortex. Helical strake (Trim *et al*., 2005; Korkischko & Meneghini, 2010), as a way of disturbance on spanwise uniformity of vortex shedding, is the most widely used at present. Similarly, triple-starting helical grooves was reported as a new method in VIV suppression and drag reduction (Huang, 2011). More information about them can be found out in reviews of Sarpkaya & Isaacson (1981), Kumar *et al*.(2008), and Wu & Sun (2009).

However, as for pre-designed flexible risers in complex ocean environment, there are always some limitations in applying these methods. Meantime, another way was proposed by introducing three-dimensional geometric disturbance, such a wavy front surface (Bearman & Owen, 1998), and totally wavy cylinders (Owen *et al*., 1999; Lin *et al*., 2010). However, these disturbances were introduced in a streamwise-spanwise plane and thus sensitive to the flow direction. Then a new idea was generated (Lin *et al*., 2011), based on the Bernoulli equation and the effect of geometric disturbance on flow field. But different from previous methods, such disturbance was introduced in a radial-spanwise plane. At least, initial experiments have shown that the new disturbance does reduce the oscillating amplitude at certain waviness at the start of synchronization. Nevertheless, related investigations for other features of such disturbances on VIV have not finished yet.

In present paper, the main purpose is to exploit features of VIV responses of amplitude and frequency for the circular cylinder with two types of geometric disturbances, harmonic and cone-like. Firstly, experiments instruments are illustrated in detail. Then experimental results by the pendulum oscillated in water channel are presented and analyzed. At last, the conclusions are given.

EXPERIMENTAL DETAILS

The experiments were conducted in a circulating water channel, as shown in Fig. 1, at Key Laboratory for Hydrodynamics and Ocean Engineering, Institute of Mechanics, Chinese Academy of Sciences. The test section was 6 m long and 1 m wide. Here the water depth was 0.7 m. The flow was bi-directionally driven by an electronic bump adjusted from a remote computer. The maximum speed could be reached up to 1 m/s.

Figure 1. Water channel in VIV experiments

Experimental instruments with oscillating cylinders were shown in Fig. 2. The whole cylinder with specific disturbance was installed through the circular hole on the flat plate with the diameter greater than the maximum diameter of cylinder, and supported by the equilateral triangle iron support installed conversely with one apex as the support point. Such iron support was rotatable due to its sharp edge touched to the platform. The cylinder fixed with such support would be oscillated along a direction perpendicular to the direction of support, which was parallel to the flow direction. The restoration came from the gravity of whole oscillating cylinder, just like a pendulum. The platform could be adjusted to keep the plate in the horizontal level by the screws. The whole frame was mounted across the channel.

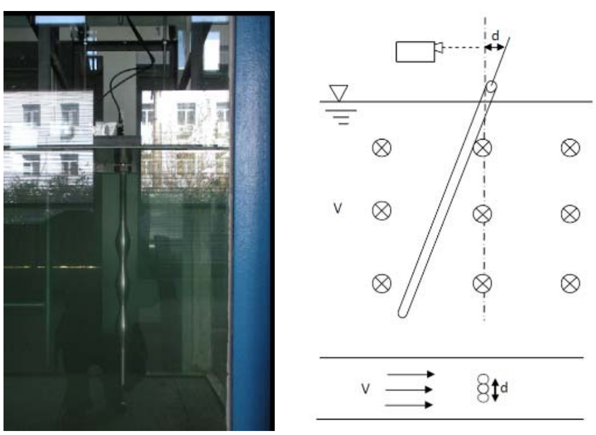

(a) (b)

Figure 2. (a) Oscillating cylinder with harmonic disturbance installed on the platform; (b) schematic of cylinder oscillated transversely.

The whole oscillating structure was mainly composed of overwater, test and underwater sections. The overwater section included the indicating arm, used to receive the laser beam launched from the laser displacement sensor, the equilateral triangle iron support and a straight cylinder with the length of 100 mm. In the underwater section, two auxiliary straight cylinders, same as one used in the overwater section, were designed in avoiding effects of wave, free surface and bottom of channel at high incoming velocities. Test sections with straight or wavy shapes were manufactured as three parts connected by inner screws. Each part was 120 mm long. The immersed length of whole cylinder was then 560 mm. All these sections were made up to aluminum with same outer diameter of 20 mm and inner diameter of 10 mm. Presently as for two types of wavy cylinders, as shown in Fig. 3, three different waviness, 0.025, 0.05 and 0.1, were studied with the prescribed wavelength of 120 mm. The maximum outer diameters were consequently obtained as 26, 32 and 44 mm, respectively.

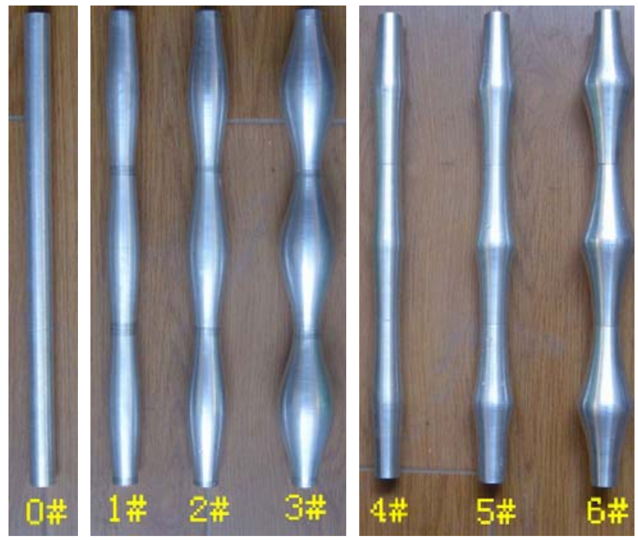

(a) (b) (c)

Figure 3. (a) Straight, (b) harmonic and (c) cone-like cylinders in test sections.

The mass of those cylinders and mass ratio of whole structure, non-dimensionalized by the mass of water with same displacement volume of straight cylinder with immersed length, were listed in Table 1. The mass ratio of whole oscillating structure kept lower.

Table 1. Mass and mass ratio of oscillating cylinders in experiments.

Number of cylinder	Mass* (g) (growth rate)	Mass (g) (growth rate)	Mass ratio
$0^{\#}$	282 (0%)	1246.35 (0%)	7.08
$1^{\#}$	382.1 (35.5%)	1346.45 (8%)	7.65
$2^{\#}$	512.5 (81.7%)	1476.85 (8%)	8.39
$3^{\#}$	817.75 (190%)	1780.1 (42.8%)	10.11
$4^{\#}$	343.6 (21.8%)	1307.95 (4.9%)	7.43
$5^{\#}$	434.2 (54%)	1398.55 (12.2%)	7.95
$6^{\#}$	681.6 (141.7%)	1645.95 (32.1%)	9.35

* Only for test sections of whole oscillating cylinder.

The uniform velocity of incoming flow was measured by the Ultrasonic Doppler speed measuring instrument. The probe was located about 5 m far away from test cylinders. The oscillating amplitudes were measured by the laser displacement sensor, which was fixed and parallel to the direction of oscillating indicating arm.

RESULTS AND ANALYSIS

Estimation of Damping

It is important for structural damping in studying VIV suppression. Sometimes, a suppressor maybe effective at high-level damping but becomes ineffective at lower-level damping. Therefore, the first experiment should be arranged in estimating the damping level by oscillating straight cylinder freely in still air.
As shown in Fig. 4, the natural frequency of decayed oscillation is 0.81 Hz. The fitting curve of local peak amplitude is thus obtained based on the following equation,

$$y(t) = \overline{y} + a\mathrm{e}^{-\zeta 2\pi f_{s0} t} \quad (1)$$

where y is the time history of displacement, y with the over line is the averaged value indicating the equilibrium position, a is an initial position of 0.653 at time of zero, ζ is the non-dimensional damping coefficient of oscillating system here, and f_{s0} is the natural frequency of body. Here ζ = 7×10^4. It shows that the damping level of present dynamic system keeps very low. Furthermore, it can be confirmed that the structural damping is also less or equal to such level.

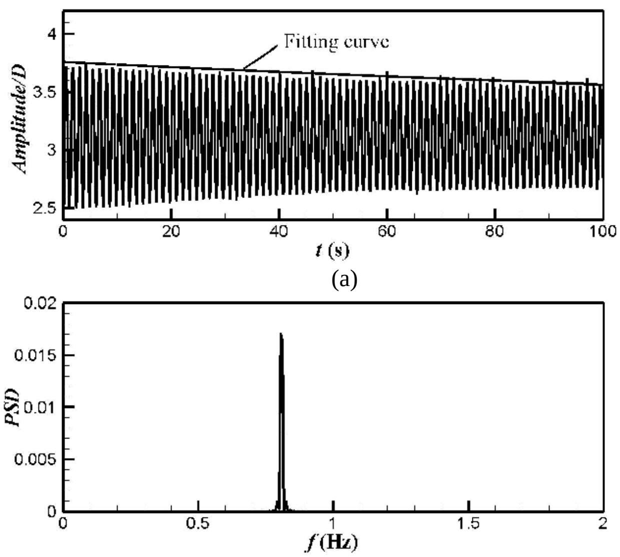

(a)

(b)

Figure 4. Experiments for free oscillation of the straight cylinder in still air, (a) displacement time history, (b) power spectral density (PSD) of lateral displacement.

Natural Frequency

Natural frequencies of cylinders with or without geometric disturbances were measured through the free vibrations in still water. The time histories of lateral displacements and frequency analysis were typically as shown in Fig. 5 for the $0^{\#}$ straight cylinder. Due to the higher viscosity of water, the oscillating amplitude was reduced quickly down to stop. Although there were many disturbed signals with large amplitudes, the natural frequency could still be identified clearly.

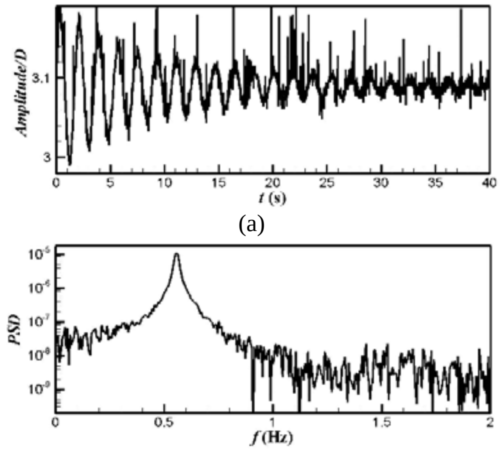

(a)

(b)

Figure 5. Experiments for free oscillation of the straight cylinder in still water, (a) transverse displacement time history and (b) PSD.

As presented in Table 2, the natural frequencies for two types of wavy cylinders are almost close or equal to that of straight cylinder. Moreover, there is no obvious change in natural frequency as the waviness increases. Hence, the geometric disturbances and variation of waviness have hardly obvious effects on the natural frequency.

Table 2. Natural frequencies of cylinders oscillated freely in still water.

Number	$0^{\#}$	$1^{\#}$	$2^{\#}$	$3^{\#}$	$4^{\#}$	$5^{\#}$	$6^{\#}$
f_{s0} (Hz)	0.56	0.56	0.56	0.56	0.55	0.55	0.55

On the other hand, based on the relationship between the Reynolds number and the Strouhal number for the fixed circular cylinder, the frequency of vortex shedding could be estimated before VIV experiments. The Strouhal number is taken from the book of Sarpkaya & Isaacson (1981). By comparing between Tables 2 and 3, it can be predicted that the start of synchronization of VIV of straight cylinder would be occurred firstly near the incoming velocity of 5 cm/s.

Table 3. The Reynolds number, Strouhal number and estimated frequencies of vortex shedding in flows around a fixed circular cylinder.

Velocity (cm/s)	5	10	15	20	25	30	40
Re	1000	2000	3000	4000	5000	6000	8000
St	0.22	0.21	0.21	0.21	0.21	0.21	0.2~0.21
f_{f0} (Hz)	0.55	1.05	1.58	2.1	2.63	3.15	4~4.2

Oscillating Amplitude

Responses of oscillating amplitudes are presented for straight and harmonic-shaped cylinders. As shown in Fig. 6, the RMS values of amplitudes are varied with the increased or decreased reduced velocity, which is defined as the incoming velocity non-dimensionalized by the natural frequency of structure. It can be seen that the straight cylinder ($0^{\#}$) is on synchronization at the range of reduced velocity from 4 to 10. Compared to the harmonic cylinders, at the start of synchronization, the amplitude is little increased at the waviness of 0.025, but reduced at the waviness of 0.05 and 0.1. The reductions are increased with the increasing waviness. The maximum of 48.5% is reached at waviness of 0.1. However, when the reduced velocity increases up to near 10, the oscillating amplitude of wavy cylinders increases with the increasing waviness, and becomes greater than hat of straight cylinder. Moreover, the region of synchronization seems to be enlarged because of the end of synchronization extending to greater reduced velocity. Correspondingly, the peak amplitude, appeared at the start of synchronization for the straight cylinder, moves towards the greater reduced velocity for the disturbed cylinders. The maximum of increasing amplitude is 101% at waviness of 0.1.

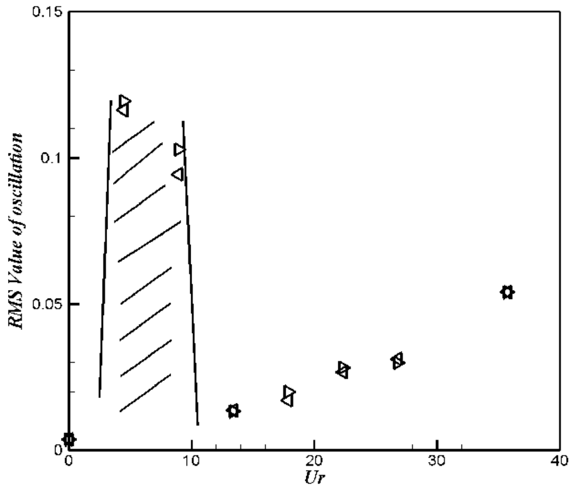

(a)

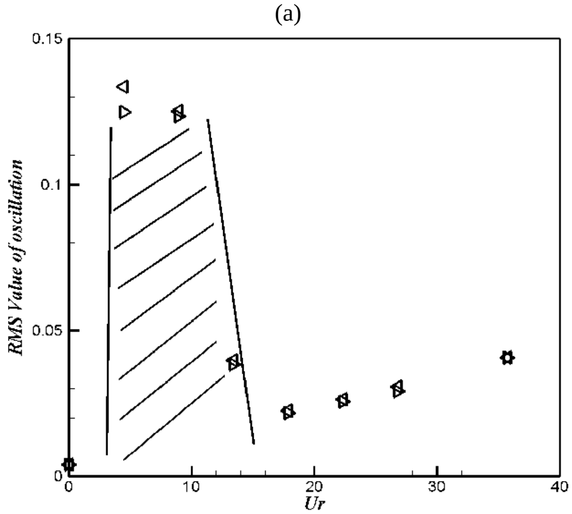

(b)

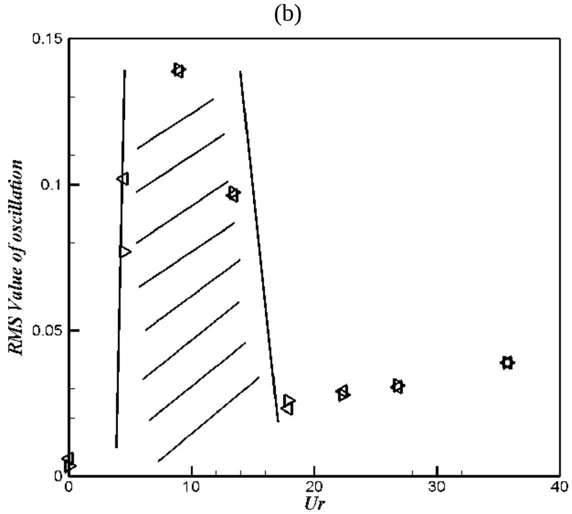

(c)

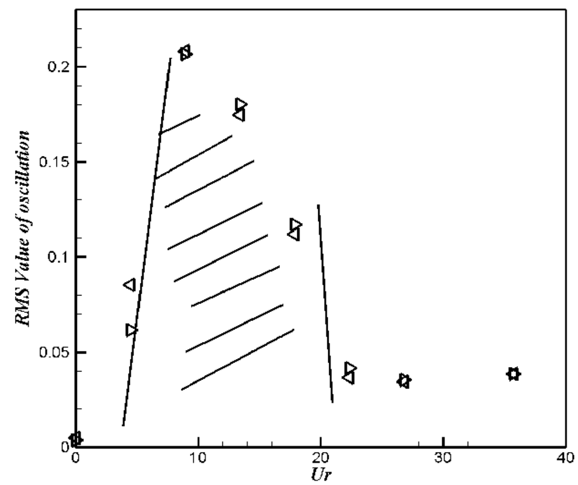

(d)

Figure 6. Amplitude responses, RMS values, varied with the reduced velocity, where the shadow regions estimate the occurrence of synchronization, (a) 0#; (b) 1#; (c) 2#; (d) 3#, where ▹ and ◃ denote the increasing and decreasing reduced velocities.

On the other hand, RMS values with the increasing reduced velocity are less different from those with the decreasing reduced velocity. But such difference becomes obviously great for the harmonic cylinder at the start of synchronization, even reaching up to about 30%. Such phenomenon may be related to the hysteresis.

As for the cone-like cylinders, the characteristics of amplitude responses are similarly. As shown in Fig. 7, the waviness of 0.05 and 0.1 and only variation with the increasing reduced velocity are presented. More trivial velocity interval is adopted. The amplitude reduction at the start of synchronization reaches up to 53.2% at waviness of 0.1. And the maximum increase of amplitude is 77.2% at waviness of 0.1 and incoming velocity of 10 cm/s.

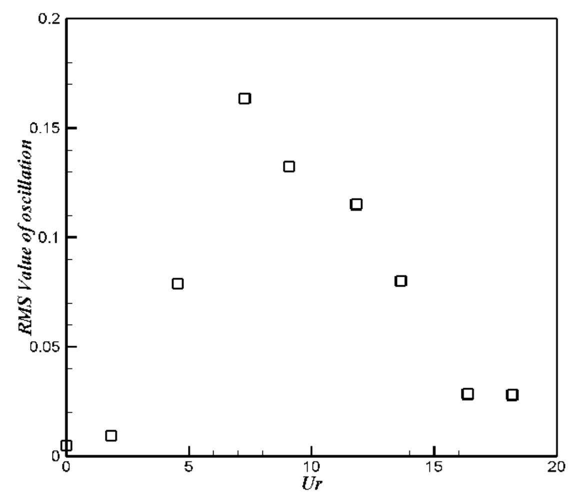

(a)

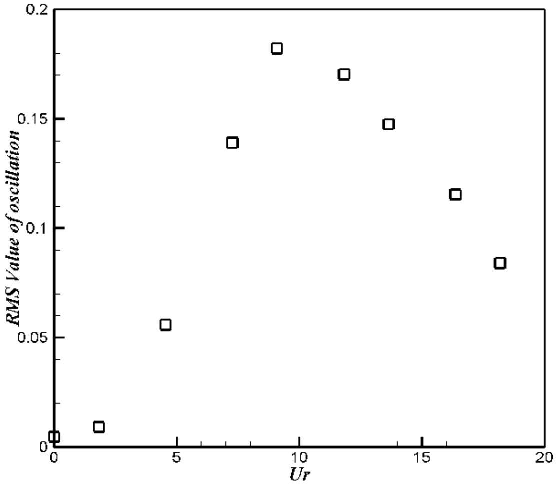

(b)

Figure 7. Amplitude responses of cone-like cylinders, RMS values, varied with the increasing reduced velocity, (a) $5^{\#}$; (b) $6^{\#}$.

The increasing amplitude response for disturbed cylinders at higher reduced velocities could be related with the disruption in effects of geometric disturbances on flow. Furthermore, it should be emphasized here in present experiments that the VIV of pendulum is significantly different from that of the flexible riser in deep sea in two aspects. One is that the pendulum is rigid, while riser is flexible due to its large aspect ratio. Therefore, oscillating amplitudes would be varied along the span. Another is the different boundary conditions at ends of cylinder. For the risers, both ends are limited to be moved or rotated, rather than freely moved for one end of pendulum. This is very important in the dynamics because the gravity would be ignored in the flexible risers where the top tension becomes principle.

Those features above have been also confirmed from the time histories of oscillating amplitudes in steady status. As shown in Fig. 8, the straight cylinder ($0^{\#}$), the harmonic cylinder with waviness of 0.1 ($3^{\#}$) and the cone-like cylinder with waviness of 0.05 ($5^{\#}$) are presented. It can be shown that the envelopes of local peak amplitude are varied wavily along the time, especially near the end of synchronization. Outside of synchronization, all cylinders are oscillated chaotically with little amplitudes.

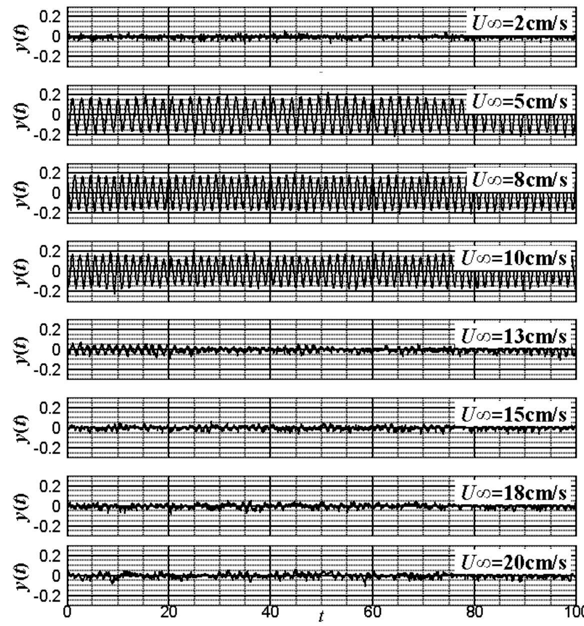

(a)

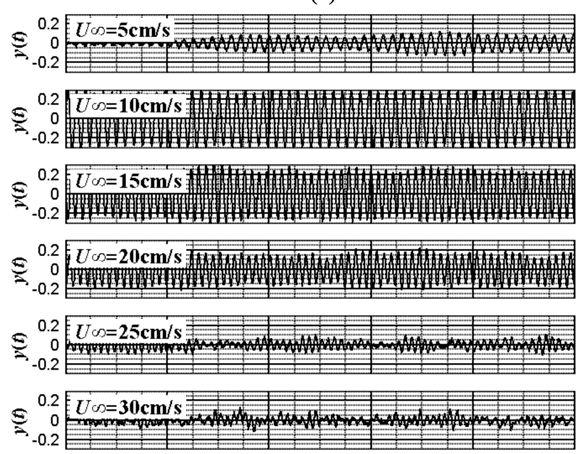

(b)

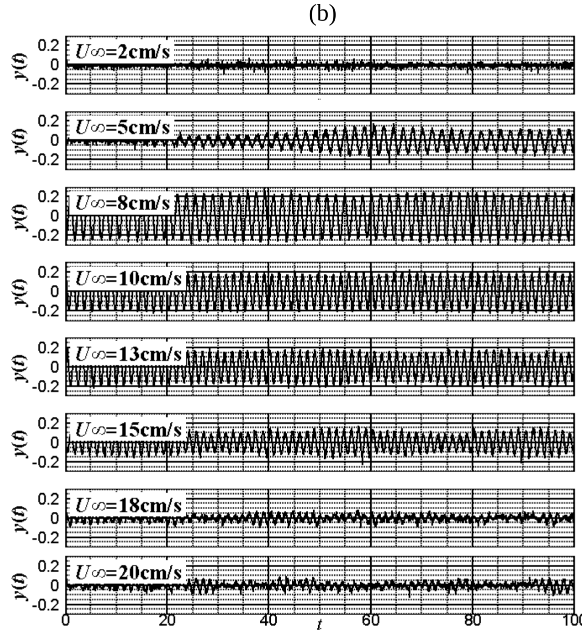

(c)

Figure 8. Time histories of oscillating amplitudes for (a) $0^{\#}$, (b) $3^{\#}$ and (c) $5^{\#}$ cylinders at different incoming velocities, respectively.

Oscillating Frequency

At the region of synchronization, the cylinder is oscillated by the single frequency. Outside of synchronization, the cylinder is oscillated with small amplitude, and there is no main frequency dominated. Therefore, the frequency ratio of the oscillating frequency to the natural frequency varied with the reduced velocity for different cylinders could be presented, as shown in Fig. 9. All oscillating frequencies are increased on synchronization. Especially at higher reduced velocities, the frequency ratio exceeds 1 over the percentage of 20 to 30, rather than almost near 1 in VIV of a two-degree-of-freedom circular cylinder. Such phenomenon demonstrates the oscillation of disturbed cylinder is greatly affected by the incoming flow at higher vortex shedding frequency.

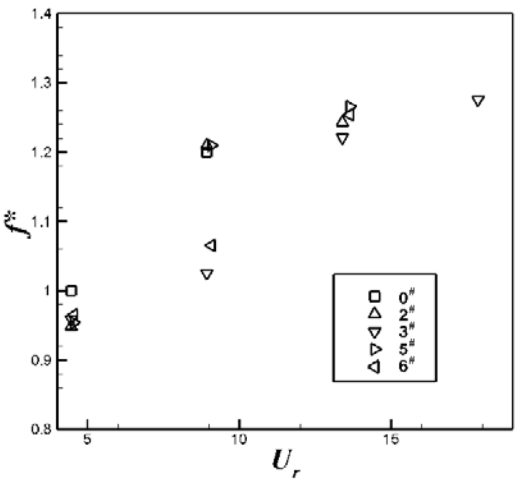

Figure 9. Oscillating frequency ratio varied with the reduced velocity on synchronization for different cylinders.

Through the Morlet wavelet analysis, as shown in Fig. 10, features of the wavy variation of peak amplitude on synchronization are represented by intermittent magnification of PSD. And during the whole experimental time, the cylinder does oscillate by a single frequency. Outside of synchronization, chaotic behaviors with little amplitudes are reflected by the multi-frequency, which are suddenly appeared at the same time, and discontinue variation of PSD along the time.

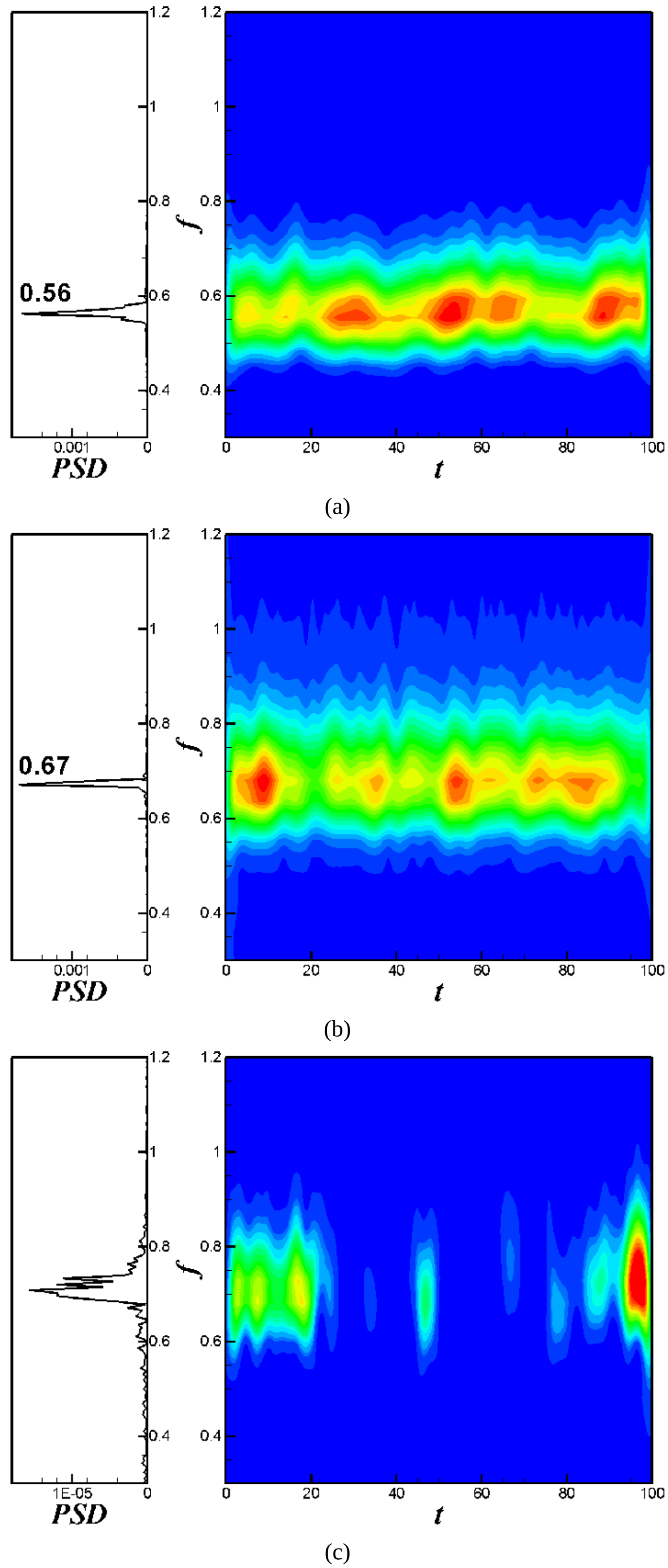

Figure 10. Frequencies and the Morlet wavelet analysis for the straight cylinder at different incoming velocities, (a) 5 cm/s, (b) 10 cm/s and (c) 13 cm/s.

CONCLUSIONS

On the previous work, a new device in suppressing VIV by wavy geometric disturbances in a radial-spanwise plane was proposed. Then in present paper, the VIV experiments are quickly carried out through the oscillation of pendulum at different incoming velocities. With the aim to obtain the effect of disturbances on VIV, two patterns of wavy shapes, harmonic and cone-like, are selected and three waviness of 0.025, 0.05 and 0.1 are considered with the non-dimensional wavelength of 6.

The oscillating amplitudes are all amplified greatly during the lock-in. The phenomenon, similar to the hysteresis, is appeared for the disturbed cylinders at the start of synchronization, but not observed in the VIV of straight cylinder. After introducing disturbances, the peak amplitude is increased with the increasing waviness. The region of synchronization is also enlarged down to higher reduced velocities. At the start of synchronization, the oscillating amplitude is really reduced. The maximums reach up to 48.5% and 53.2% for the harmonic and cone-like cylinders at waviness of 0.1, respectively. However, at higher reduced velocity, the increase of amplitudes reaches up to 101% and 77.2%. On the other hand, the wavy variation of amplitude is observed, especially near the end of synchronization. On synchronization, the cylinder is oscillated with the single frequency, which is increased as the reduced velocity increases.

From the variation of oscillating amplitude along the reduced velocity, these two types of geometric disturbances at least succeed in delaying the magnified oscillating amplitude down to higher velocity, although the oscillation becomes more violently than that of straight cylinder at higher reduced velocity. This gives us a new hope in improving such design in future study. Considering the pendulum obviously different from the flexible riser in fluid-structure coupled dynamics, there are a lot of works to be done in obtaining a suitable VIV suppressor, such as hydrodynamic experiments in one or two-degree-of-freedom VIV, and coupled with the in-line VIV.

ACKNOWLEDGEMENTS

The authors sincerely acknowledge the support of the Knowledge Innovation Program of Chinese Academy of Sciences under Grant No KJCX2-YW-L02, and the Important National Science & Technology Specific Projects of Grant No 2008ZX05056-03-06 for the work reported in this paper.

REFERENCES

Bearman, PW, and Owen, JC (1998). "Reduction of bluff-body drag and suppression of vortex shedding by the introduction of wavy separation lines," *J Fluids Struct*, Vol 12, pp 123-130.

Gabbai, RD, and Benaroya, H (2005). "An overview of modeling and experiments of vortex-induced vibration of circular cylinders, " *J Sound Vib*, Vol 282, pp 575-616.

Huang, S (2011). "VIV suppression of a two-degree-of-freedom circular cylinder and drag reduction of a fixed circular cylinder by the use of helical grooves," *J Fluids Struct*, Vol 27, pp 1124-1133.

Korkischko, I, and Meneghini, JR (2010). "Experimental investigation of flow-induced vibration on isolated and tandem circular cylinders fitted with strakes," *J Fluids Struct*, Vol 26, pp 611-625.

Kumar, RA, Sohn, CH, and Gowda, BHL (2008). "Passive control of vortex-induced vibrations: an overview," *Recent Patents on Mechanical Eng*, Vol 1, No 1, pp 1-11.

Lee, L, and Allen, DW (2005). "The dynamic stability of short fairings," *Offshore Tech Conf Houston*, Texas, USA, OTC 17125.

Lin, LM, Ling, GC, and Wu, YX (2010). "Mechanism responsible for the complete suppression of Karman vortex in flows past a wavy square-section cylinder," *Chin Phys Lett*, Vol 27, No 3, pp 034702.

Lin, LM, Zhong, XF, and Wu YX (2011). "Experimental investigation of a new device in suppressing vortex-induced vibrations of a circular cylinder," *Proc 21st Int Offshore and Polar Eng Conf*, ISOPE, Maui, pp 1283-1288.

Owen, JC, Szewczyk, AA, and Bearman, PW (1999). "Suppressing Kármán vortex shedding by use of sinuous circular cylinders," *Bulletin of the American Physical Society*, Vol 44, pp 124.

Owen, JC, Bearman, PW, and Szewczyk, AA (2001). "Passive control of VIV with drag reduction," *J Fluids Struct*, Vol 15, pp 597-605.

Sarpkaya, T (1979). "Vortex-Induced Oscillations—A Selective Review, " *J Appl Mech*, Vol 46, pp 241-258.

Sarpkaya, T (2004). "A critical review of the intrinsic nature of vortex-induced vibrations, " *J Fluids Struct*, Vol 19, pp 389-447.

Sarpkaya, T, and Isaacson, M (1981). *Mechanics of wave forces on offshore structures*. Van Nostrand Reinhold Company, 606pp.

Song, JN, *et al*. (2009). "Experimental investigation of suppression of vortex-induced vibration of marine risers by three control rods," *Ocean Eng*, Vol 27, No 3, pp 23-29.

Trim, AD, Braaten, H, Lie, H, and Tognarelli, MA (2005). "Experimental investigation of vortex-induced vibration of long marine risers," *J Fluid Struct*, Vol 21, pp 335-361.

Williamson, CHK, and Govardhan, R (2004). "Vortex-induced vibrations, " *Annu Rev Fluid Mech*, Vol 36, pp 413-455.

Wu, H, and Sun, DP (2009). "Study on suppression measures for vortex-induced vibration of the deepwater riser," *China Offshore Platform*, Vol 24, pp 1-8.